Acta Pharmaceutica Sinica B 2017;7(3):390–394

Chinese Pharmaceutical Association
Institute of Materia Medica, Chinese Academy of Medical Sciences

Acta Pharmaceutica Sinica B

www.elsevier.com/locate/apsb
www.sciencedirect.com

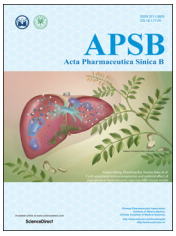

SHORT COMMUNICATION

Structural analysis of recombinant human ubiquitin-conjugating enzyme UbcH5c

Fangshu Wu, Junsheng Zhu, Honglin Li*, Lili Zhu*

Shanghai Key Laboratory of New Drug Design, School of Pharmacy, East China University of Science and Technology, Shanghai 200237, China

Received 23 October 2016; received in revised form 4 December 2016; accepted 19 December 2016

KEY WORDS

UbcH5c;
NF-κB;
Ubiquitination;
Ubiquitin-conjugating enzyme;
Crystal structure;
Inflammatory target

Abstract UbcH5c belongs to the ubiquitin-conjugating enzyme family and plays an important role in catalyzing ubiquitination during TNF-α–triggered NF-κB activation. Therefore, UbcH5c is a potent therapeutic target for the treatment of inflammatory and autoimmune diseases induced by aberrant activation of NF-κB. In this study, we established a stable expression system for recombinant UbcH5c and solved the crystal structure of UbcH5c belonging to space group $P22_12_1$ with one molecule in the asymmetric unit. This study provides the basis for further study of UbcH5c including the design of UbcH5c inhibitors.

*Corresponding authors. Tel.: +86 21 64253379.
E-mail addresses: hlli@ecust.edu.cn (Honglin Li), zhulfl@ecust.edu.cn (Lili Zhu).

Peer review under responsibility of Institute of Materia Medica, Chinese Academy of Medical Sciences and Chinese Pharmaceutical Association.

http://dx.doi.org/10.1016/j.apsb.2016.12.008

1. Introduction

Nuclear factor kappa enhancer binding protein (NF-κB) is a family of transcription factors and highly involved in a variety of biological processes including inflammation, immune response and apoptosis[1,2]. In the tumor necrosis factor (TNF-α)/NF-κB pathway, TNF-α initiates the NF-κB pathway by binding to TNF receptor–associated death domain protein (TRADD), which recruits receptor-interacting protein 1 (RIP1) and TNF receptor-associated factor 2 (TRAF2). Then TRAF2 can recruit cellular inhibitor of apoptosis proteins 1 and 2 (c-IAP1 and 2)[3]. c-IAP1 and 2 function as the key ubiquitin-protein ligases (E3s) which induce RIP1 ubiquitination[4]. Subsequently, NF-κB essential modifier (NEMO) binds to polyubiquitinated RIP1, and recruits the inhibitors of NF-κB kinase (IKK) complexes in order to facilitate its activation[5,6]. Once activated, IKK is able to phosphorylate the inhibitors of NF-κB (IκB) and allows it to be destroyed by the 26 S proteasome. And then, free NF-κB is liberated to enter the nucleus and activates transcription of downstream genes involved in inflammatory and immune responses[2,7].

In TNF-α–triggered NF-κB pathway, ubiquitination is directly involved in NF-κB activation, such as proteasomal degradation of IκB and activation of IKK complexes. Therefore, ubiquitination plays an essential role in the regulation of NF-κB pathway[8]. In ubiquitination pathway, at least three classes of enzymes are involved in the conjugation of ubiquitin (Ub) to specific proteins. Firstly, ubiquitin-activating enzyme (E1) forms a high energy thiol ester bond between the C-terminus of Ub and a cysteine of E1 in an ATP-dependent reaction. Next, ubiquitin-conjugating enzyme (E2) acquires the activated Ub through a *trans*-thioesterification reaction. Finally, E2 enzymes either by themselves or in combination with E3 transfer Ub monomers or multiubiquitin chains to target proteins, where stable isopeptide linkages are formed[9,10].

Several E2s, such as UbcH5 and Ubc13, are involved in the NF-κB pathway[1,11]. UbcH5 belongs to E2 family and is composed of UbcH5a, UbcH5b and UbcH5c[12]. UbcH5 is critical regulator of the stability of c-IAP1 which promotes polyubiquitination of RIP1 *in vitro* and *in vivo*[13]. In addition, UbcH5 is indispensable for IKK activation which promotes the phosphorylation of IκB and liberates NF-κB[12,14]. Moreover, the cells knocking out of UbcH5 are able to inhibit IKK activation[15]. Consequently, UbcH5 plays an important role in TNF-α–triggered NF-κB pathway. According to the previous report, IJ-5 was discovered as a potential inhibitor of UbcH5c, which exhibited anti-inflammatory activity against TNF-α– and D-galactosamine–induced hepatitis and collagen-induced arthritis[16]. Therefore, UbcH5c may serve as a potent therapeutic target for the treatment of inflammatory and autoimmune diseases induced by aberrant activation of NF-κB. Here, the expression, purification, crystallization, X-ray diffraction and structure determination studies of UbcH5c are described.

2. Materials and methods

2.1. Materials

Complementary deoxyribonucleic acid (cDNA) encoding UbcH5c was purchased from FulenGen Co., Ltd. (Guangzhou, China). The primers were synthesized from Sunny Biotechnology Co., Ltd. (Shanghai. China). pET-28a vector was saved by the laboratory, and *Escherichia coli* BL21 (DE3) competent host cells and plasmid extraction kit were purchased from Tiangen Biotech Co., Ltd. (Beijing, China). Restriction enzymes and Taq DNA polymerase were purchased from New England Biolabs (Beijing) Ltd. The columns used in this study from General Electric Company (USA). All other fine chemicals and reagents were of analytical grade and commercial available.

2.2. Expression and purification of UbcH5c

The gene encoding UbcH5c was inserted into the pET-28a vector with a noncleavable N-terminal hexahistidine tag (Table 1). The construct was verified by sequencing and transformed by heat shock into *E. coli* BL21 (DE3) competent host cells.

The transformant containing the target plasmid was grown overnight on Luria-Bertani (LB) medium containing 100 μg/mL kanamycin at 310 K, which was used as a 1% (*v*/*v*) inoculum for 4 L LB-kanamycin expression cultures. Then 4 L cultures were incubated at 310 K until that the value of OD_{600} was reached to 0.8 and induced by the addition of 0.5 mmol/L isopropyl β-D-1-thiogalactopyranoside (IPTG). After incubation for an additional 18 h at 289 K, the cells were harvested by centrifugation and then stored at 203 K for further use.

For the purification of His_6-UbcH5c, the cells were thawed on ice and resuspended in buffer A (50 mmol/L HEPES, 150 mmol/L NaCl 10 mmol/L imidazole pH 7.0, 1% (*v*/*v*) Triton X-100). The

Table 1 Macromolecule production information.

Source organism	Homo sapiens
Forward primer	5′-AAAACCATGGGC*CATCATCATCATCATCAC*GGCATGGCGCT-GAAACG-3′ (*Nco* I)
Reverse primer	5′-CCGCTCGAGTCACATGGCATACTTCTGAGTCCATTCCCGAGA-TATT-3′ (*Xho* I)
Vector	pET-28a
Expression host	*E. coli* BL21 (DE3)
Complete amino acid sequence of the construct produced[a]	MGHHHHHHGMALKRINKELSDLARDPPAQCSAGPVGDDMFHW-QATIMGPNDSPYQGGVFFLTIHFPTDYPFKPPKVAFTTRIYHP-NINSNGSICLDILRSQWSPALTISKVLLSICSLLCDPNPDDPLV-PEIARIYKTDRDKYNRISREWTQKYAM

[a]The N-terminal His_6 tag is underlined.

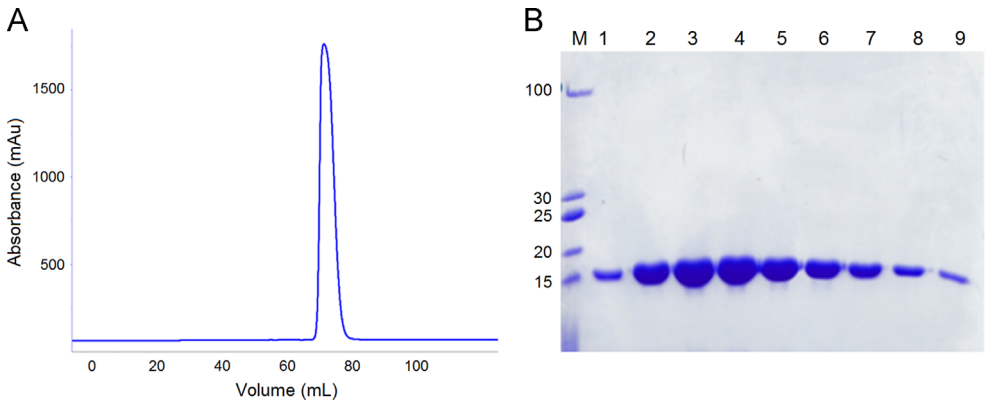

Figure 1 (A) Size exclusion chromatography for the analysis of UbcH5c; (B) SDS-PAGE analysis of purification of UbcH5c.

cell resuspension solution was disrupted by sonication on ice. The cell debris was removed from the crude extract by centrifugation at 25,000 × *g* for 30 min at 277 K, and the supernant was loaded onto a HiTrap Chelating 5 mL column (GE Healthcare) for purification by immobilized metal-affinity chromatography (IMAC). The nonspecifically bound proteins were removed by washing with five column volumes (CV) of buffer A. The recombinant protein was eluted with a linear gradient (10 – 500 mmol/L) of imidazole. Fractions containing UbcH5c were pooled and then ethylenediaminetetraacetic acid (EDTA) and dithiothreitol (DTT) were added into the pool to the concentration of 1 and 2 mmol/L, respectively. The pooled fractions were concentrated to 5 mL and diluted with buffer B (30 mmol/L MES pH 6.0, 30 mmol/L NaCl, 2 mmol/L DTT) to 30 mL. Then the sample was loaded on a Hitrap SP FF 5 mL column (GE Healthcare) equilibrated with buffer B. The column was washed with 30 CV of a linear gradient of NaCl (30 – 500 mmol/L). The eluted protein was pooled, concentrated and loaded on a Superdex 75 16/60 column (GE Healthcare) equilibrated with buffer C (50 mmol/L HEPES pH 7.0, 150 mmol/L NaCl). Fractions containing UbcH5c were concentrated to 10 mg/mL for crystallization.

2.3. *Crystallization of UbcH5c*

Initial crystallization experiments were carried out with five commercial crystallization screens from Hampton Research (Index HT, Crystal Screen HT, PEG/Ion HT, PEGRx HT and SaltRx HT). All initial screens were performed using a protein concentration of 10 mg/mL and the hanging-drop vapour-diffusion method in 24-well plates at 293 K. Protein solution (1 µL) was mixed with 1 µL reservoir solution and equilibrated against 500 µL reservoir solution.

2.4. *Data collection and processing*

Crystals of UbcH5c were briefly soaked in mother liquor supplemented with 25% glycerol as a cryoprotectant. Crystals were then flash-cooled to 100 K in liquid nitrogen. X-ray diffraction data were collected at 100 K on beam line BL17U1 at the Shanghai Synchrotron Radiation Facility (SSRF). A total of 270 images were collected using an oscillation range of 1.0°. The raw data were processed using MOSFLM and SCALA program from CCP4 suite[17,18]. The initial phase was obtained *via* the molecular-replacement method. The model was chosen from protein data bank (PDB) entry 1x23. The structure of UbcH5c protein was refined using *REFMAC*[19]. After cycles of refinement and model building with *Coot*[20], the molecular graphics were prepared with PYMOL (DeLano, 2002) to generate the figures.

3. Results and discussion

In this study, UbcH5c was cloned, overexpressed using an *E. coli* expression system and purified to homogeneity (Fig. 1A and B). A single peak was obtained with an elution volume corresponding to 17.8 kDa. The purified recombinant UbcH5c was produced with a yield of 80 mg/L. After initial crystallization experiments with five commercial crystallization screens from Hampton Research, we found two hits of crystallization conditions from the initial screens: (i) 0.2 mol/L sodium malonate pH 4.0, 20% *w/v* polyethylene glycol 3350 and (ii) 2% *v/v* tacsimate pH 4.0, 0.1 mol/L sodium acetate trihydrate pH 4.6, 16% *w/v* polyethylene glycol 3350. In condition (i), crystals piled up together and they were relatively small. In condition (ii), initial crystals diffracted very poor. Further optimization of these two conditions was performed using the hanging-drop vapour-diffusion technique in 24-well plates at 293 K by varying the polyethylene glycol concentration and pH. Crystals suitable for X-ray diffraction appeared in 2 weeks (Fig. 2). Composition of reservoir solution is 2% *v/v* tacsimate pH 4.0, 0.1 mol/L sodium acetate trihydrate pH 4.8, 20% *w/v* polyethylene glycol 3350.

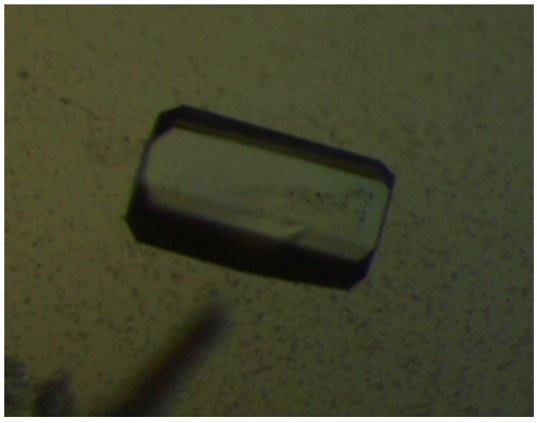

Figure 2 One crystal of UbcH5c grown at 293 K (100 ×).

Table 2 Data collection and refinement statistics for UbcH5c crystal structure.

Diffraction source	BL17U1 beamline, SSRF
Wavelength (Å)	0.9792
Temperature (K)	100
Detector	ADSC Q315r
Crystal-detector distance (mm)	230
Rotation range per image (°)	1
Total rotation range (°)	270
Space group	P 2 2_1 2_1
a, *b*, *c* (Å)	28.170, 66.280, 76.740
α, β, γ (°)	90.00, 90.00, 90.00
Mosaicity (°)	0.50
Resolution range (Å)	30.42–1.76
Total No. of reflections	196803 (29092)
No. of unique reflections	14838 (2116)
Completeness (%)	99.6 (100.0)
Redundancy	13.3 (13.7)
R_{merge} (%)[a]	12.7 (34.4)
I/σ (I)[b]	12.1 (5.5)
Overall *B* factor from Wilson plot (Å^2)	21.72
R/R_{free} (%)[c]	20.6/25.2
Bonds (Å)	0.011
Angles (deg.)	1.316
PDB code	5egg

[a]$R_{merge} = 100 \times \Sigma_h \Sigma_j |I_{h,j} - I_h| / \Sigma_h \Sigma_j I_{h,j}$ where I_h is the weighted mean intensity of the symmetry-related refractions $I_{h,j}$.

[b]Values for the outermost resolution shell are given in parentheses.

[c]R_{free} is calculated using a randomly selected 5% sample of reflection data omitted from the refinement.

The crystal of UbcH5c diffracted to 1.76 Å resolution and belonged to space group P22$_1$2$_1$, with unit-cell parameters a = 28.17, b = 66.28, c = 76.74 Å, α = 90.0, β = 90.0, γ = 90.0°. One UbcH5c molecule was found in the asymmetric unit with a Matthews coefficient of 2.17 Å^3/Da, corresponding to a solvent content of 43.25%. The crystal structure of UbcH5c was determined by molecular replacement and the final refinement produced R and R_{free} values of 20.6% and 25.2%, respectively. The coordinates had been deposited in the PDB data bank as PDB entry 5egg. The data quality and model refinement statistics are presented in Table 2.

About the crystal structure of UbcH5c determined in this study, electron density is visible for residues 1–147 and one extra glycine (G0) from the vector. UbcH5c is comprised of an N-terminal α-helix (α1, 1–15), a four-strand forming antiparallel β-sheet (β1, 22–24; β2, 32–38; β3, 49–55 and β4, 66–69), a 3/10 α-helix (3/10 α, 87–89) close to the active site (C85), and an additional three α-helices (α2, 99–111; α3, 121–129 and α4, 131–145) (Fig. 3A and B).

The crystal structure of UbcH5c determined in this study has been deposited in the PDB data bank (PDB ID: 5egg). In the PDB data bank, there is another one structure of UbcH5c (PDB ID: 1x23) without published literatures. In 1x23, the crystal structure contains four UbcH5c molecules per asymmetric unit and belongs to space group P12$_1$1, while the structure of 5egg solved in this study contains one UbcH5c molecule in one asymmetric unit and belongs to space group P22$_1$2$_1$. Alignment of the chain A of 5egg with the chains A, B, C and D of 1x23 show that the C_α positions could be superimposed with an rmsd of 0.730, 0.697, 0.646 and 0.663 Å, respectively. The large variations occur in α1, β1 and L1, which are far away from the active site C85 (Fig. 4). These N-terminus regions in 1x23 are relatively compact to avoid collisions between molecules because there are four molecules in an asymmetric unit. The reasons that caused differences between the two structures may be ascribed to their different space groups with individual molecular arrangements. Compared with 1x23, α1 and β1 in 5egg slightly extend outwards from the core structure; moreover, β1 in 5egg is obviously shorter with the lack of two amino acid residues. Secondary structures including β2, β3, β4, 3/10 α, α2, α3 and α4 are well superimposed. So the whole structure of UbcH5c is relatively rigid.

In ubiquitination pathway, a thioester-linked conjugate between the C-terminus of Ub and the active site cysteine (C85) of UbcH5c is formed, and then downstream-signalling pathways are activated which regulate numerous cellular processes[10]. Recently, it was reported that IJ-5 directly binds to and inactivates UbcH5c in cells, and exerts anti-inflammatory effects *in vivo*, which further validates UbcH5c as a therapeutic target for anti-TNF-α interventions[16]. Therefore, development and discovery of UbcH5c inhibitors will provide new anti-inflammatory agents. Through analysis of the crystal structure of UbcH5c solved by us, we found one shallow groove around the active site which is formed by residues C85, L86, D87, R90, S91, Q92, N114 and D117 (Fig. 5). So in the

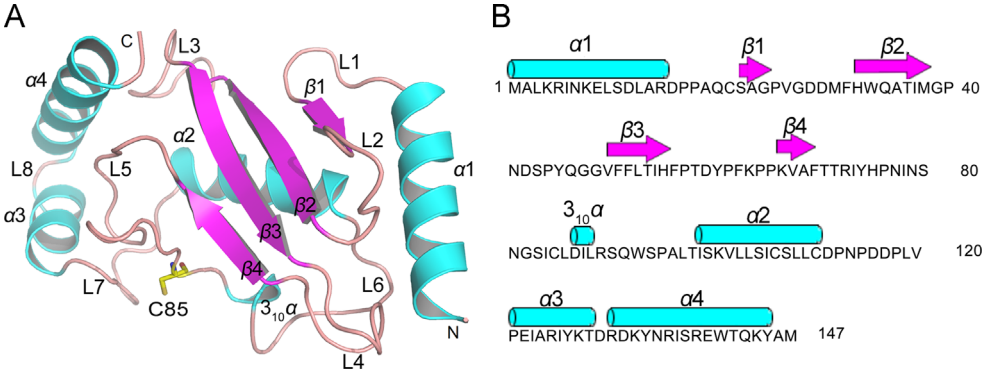

Figure 3 Overall view of the structure of UbcH5c. (A) Cartoon representation of the UbcH5c. The N and C termini of UbcH5c are labeled N and C. Secondary structure elements of UbcH5c are labeled α (cyan), β (magenta) and L (pink). The active site (C85) is shown as sticks. (B) Secondary structure of the UbcH5c is shown as the amino acid sequence. Bars (cyan) indicate helix and arrows (magenta) indicate β-strand.

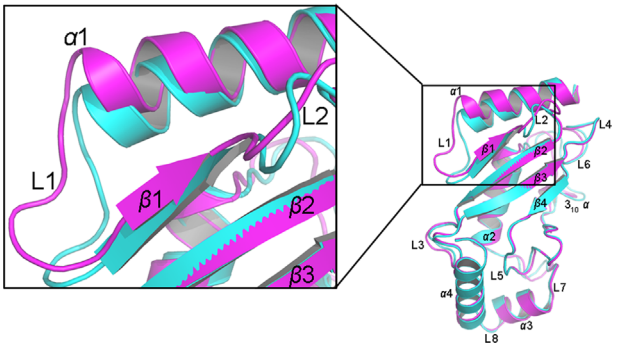

Figure 4 Superimposition of the structures between the PDB entry 5egg (magenta) and the chain A of PDB entry 1x23 (cyan). The active site (C85) is shown as sticks.

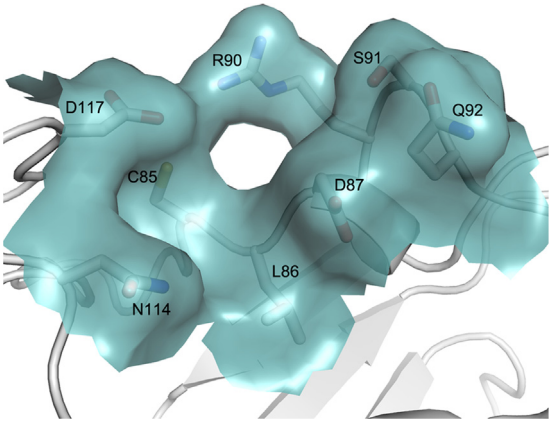

Figure 5 Details of the active site environment in the crystal structure of UbcH5c.

design process of new inhibitors of UbcH5c, a covalent bond between inhibitors and C85 *via* Michael addition can be considered. Also, hydrogen bond interactions with polar residues (D87, R90, S91, Q92, N114 or D117) are important for inhibitors binding to UbcH5c.

4. Conclusions

In this study, we successfully established the conditions of expression, purification and crystallization of UbcH5c, which provides a platform for further study of UbcH5c. In the analysis of crystal structure, we found that the structure of UbcH5c is relatively stable especially the active site, and there are several polar residues around the active site C85 forming a shallow groove. These results will provide the structural basis for the optimal design of UbcH5c inhibitors.

Acknowledgments

This work was supported by the National Natural Science Foundation of China (grants 21372078, 81302697 and 81230090), the National S&T Major Project of China (grant 2013ZX09507004), the Shanghai Committee of Science and Technology (grant 14431902400) and the Fundamental Research Funds for the Central Universities.

References

1. Chen J, Chen ZJ. Regulation of NF-κB by ubiquitination. *Curr Opin Immunol* 2013;**25**:4–12.
2. Israël A. The IKK complex, a central regulator of NF-κB activation. *Cold Spring Harb Perspect Biol* 2010;**2**:a000158.
3. Chen G, Goeddel DV. TNF-R1 signaling: a beautiful pathway. *Science* 2002;**296**:1634–5.
4. Bertrand MJ, Milutinovic S, Dickson KM, Ho WC, Boudreault A, Durkin J, et al. cIAP1 and cIAP2 facilitate cancer cell survival by functioning as E3 ligases that promote RIP1 ubiquitination. *Mol Cell* 2008;**30**:689–700.
5. Ea CK, Deng L, Xia ZP, Pineda G, Chen ZJ. Activation of IKK by TNFα requires site-specific ubiquitination of RIP1 and polyubiquitin binding by NEMO. *Mol Cell* 2006;**22**:245–57.
6. Laplantine E, Fontan E, Chiaravalli J, Lopez T, Lakisic G, Veron M, et al. NEMO specifically recognizes K63-linked poly-ubiquitin chains through a new bipartite ubiquitin-binding domain. *EMBO J* 2009;**28**:2885–95.
7. Iwai K. Diverse roles of the ubiquitin system in NF-κB activation. *Biochim Biophys Acta* 2014;**1843**:129–36.
8. Skaug B, Jiang X, Chen ZJ. The role of ubiquitin in NF-κB regulatory pathways. *Annu Rev Biochem* 2009;**78**:769–96.
9. David Y, Ziv T, Admon A, Navon A. The E2 ubiquitin-conjugating enzymes direct polyubiquitination to preferred lysines. *J Biol Chem* 2010;**285**:8595–604.
10. Page RC, Pruneda JN, Amick J, Klevit RE, Misra S. Structural insights into the conformation and oligomerization of E2∼ubiquitin conjugates. *Biochemistry* 2012;**51**:4175–87.
11. Hodge CD, Edwards RA, Markin CJ, McDonald D, Pulvino M, Huen MS, et al. Covalent inhibition of Ubc13 affects Ubiquitin signaling and reveals active site elements important for targeting. *ACS Chem Biol* 2015;**10**:1718–28.
12. Jensen JP, Bates PW, Yang M, Vierstra RD, Weissman AM. Identification of a family of closely related human ubiquitin conjugating enzymes. *J Biol Chem* 1995;**270**:30408–14.
13. Dynek JN, Goncharov T, Dueber EC, Fedorova AV, Izrael-Tomasevic A, Phu L, et al. c-IAP1 and UbcH5 promote K11-linked polyubiquitination of RIP1 in TNF signalling. *EMBO J* 2010;**29**:4198–209.
14. Chen ZJ, Parent L, Maniatis T. Site-specific phosphorylation of IκBα by a novel ubiquitination-dependent protein kinase activity. *Cell* 1996;**84**:853–62.
15. Xu M, Skaug B, Zeng W, Chen ZJ. A ubiquitin replacement strategy in human cells reveals distinct mechanisms of IKK activation by TNFα and IL-1β. *Mol Cell* 2009;**36**:302–14.
16. Liu L, Hua Y, Wang D, Shan L, Zhang Y, Zhu J, et al. A sesquiterpene lactone from a medicinal herb inhibits proinflammatory activity of TNF-α by inhibiting ubiquitin-conjugating enzyme UbcH5. *Chem Biol* 2014;**21**:1341–50.
17. Battye TG, Kontogiannis L, Johnson O, Powell HR, Leslie AG. iMOSFLM: a new graphical interface for diffraction-image processing with MOSFLM. *Acta Crystallogr D Biol Crystallogr* 2011;**67**:271–81.
18. Winn MD, Ballard CC, Cowtan KD, Dodson EJ, Emsley P, Evans PR, et al. Overview of the CCP4 suite and current developments. *Acta Crystallogr D Biol Crystallogr* 2011;**67**:235–42.
19. Murshudov GN, Skubak P, Lebedev AA, Pannu NS, Steiner RA, Nicholls RA, et al. REFMAC5 for the refinement of macromolecular crystal structures. *Acta Crystallogr D Biol Crystallogr* 2011;**67**:355–67.
20. Emsley P, Lohkamp B, Scott WG, Cowtan K. Features and development of Coot. *Acta Crystallogr D Biol Crystallogr* 2010;**66**:486–501.